The hypoxia-inducible factor is stabilized in circulating hematopoietic stem cells under normoxic conditions

Claudia Piccoli[a], Annamaria D'Aprile[a], Maria Ripoli[a], Rosella Scrima[a], Domenico Boffoli[a],
Antonio Tabilio[b], Nazzareno Capitanio[a],*

[a] *Department of Biomedical Science, University of Foggia, Foggia, Italy*
[b] *Department of Internal Medicine and Public Health, Internal Medicine and Hematology Unit, University of L'Aquila, L'Aquila, Italy*

Abstract The hypoxia-inducible factor (HIF) transcriptional system enables cell adaptation to limited O_2 availability, transducing this signal into patho-physiological responses such as angiogenesis, erythropoiesis, vasomotor control, and altered energy metabolism, as well as cell survival decisions. However, other factors beyond hypoxia are known to activate this pleiotropic transcription factor. The aim of this study was to characterize HIF in human hematopoietic stem cells (HSCs) and evidence is provided that granulocyte colony stimulating factor-mobilized CD34+- and CD133+-HSCs express a stabilized cytoplasmic form of HIF-1α under normoxic conditions. It is shown that HIF-1α stabilization correlates with down-regulation of the tumour suppressor von Hippel-Lindau protein (pVHL) and is positively controlled by NADPH-oxidase-dependent production of reactive oxygen species, indicating a specific O_2-independent post-transcriptional control of HIF in mobilized HSCs. This novel finding is discussed in the context of the proposed role of HIF as a mediator of progenitor cell recruitment to injured ischemic tissues and/or in the control of the maintenance of the undifferentiated state.
© 2007 Federation of European Biochemical Societies. Published by Elsevier B.V. All rights reserved.

Keywords: Hematopoietic stem cells; HIF; pVHL; NADPH oxidase; Redox signalling

1. Introduction

Adaptation to the environmental oxygen availability is of crucial importance in controlling cellular/tissular bioenergetic homeostasis [1]. Hypoxia-inducible factor (HIF)-1 is a ubiquitously expressed master transcription factor that activates at least 70 genes in response to hypoxic conditions [2,3], which promote cell survival, proliferation, apoptosis, glucose metabolism and angiogenesis [1–4]. HIF functions as a hetero-dimer composed of two constitutively transcribed and translated subunits, HIF-1α and HIF-1β. While HIF-1β is an oxygen-independent stable protein, HIF-1α is stabilized at low O_2 concentrations (<3%) [1].

Although it is generally considered a stressful condition, hypoxia is normally present in tissular microenvironments. The O_2 concentration in bone marrow (BM) is much lower than the average O_2 level in the majority of tissues [5] and this is particularly manifested near the bone endosteum, where the hematopoietic niches are located [6]. Thus, resident hematopoietic stem cells (HSCs) can be envisaged as a specialized cell-type, well adapted to an apparently hostile milieu where, nevertheless, they undergo self-renewal [7]. Indeed, ex vivo expansion of HSCs, without the loss of their regenerative potency, is better achieved by culturing under low O_2 tension [8]. Intriguingly, in a recent cDNA microarray analysis, it has been reported that among the 50–100 most highly up-regulated genes in human embryonic, hematopoietic (CD34+ and CD133+), and mesenchymal stem cells, HIF-1α is the only up-regulated transcription factor that they have in common [9].

Following appropriate stimuli, HSCs are mobilizable from the BM and constitute a circulating reservoir that can repopulate exhausted "niches". Recent studies have indicated that tissues that have experienced an ischemic insult can recruit circulating HSCs bringing them into play to stimulate in situ neo-vasculogenesis [10]. In both cases, the homing to BM or extra-BM tissues leads HSCs to cope with a hypoxic environment.

The present study shows for the first time that primary human granulocyte colony stimulating factor (G-CSF)-mobilized HSCs express, under normoxic conditions, high levels of stable HIF-1α and that the protein stabilization is positively controlled by NADPH-oxidase-produced reactive oxygen species and by limiting expression of the von Hippel-Lindau protein (pVHL), suggesting in HSCs a more complex regulation of HIF not exclusively related to the condition of O_2 limitation [11].

Abbreviations: BM, bone marrow; CsA, cyclosporin A; DCF, dichlorofluorescein; DFX, desferrioxamine; DPI, diphenylene iodonium; EA, human endothelial hybrid cell line (Ea.hy 926); EPO, erythropoietin; G-CSF, granulocyte colony stimulating factor; HIF, hypoxia-inducible factor; HRE, hypoxia responsive element; HSC, hematopoietic stem cell; LMN, lymphomononuclear; L-NNMA, L-monomethyl-L-arginine; LSCM, laser scanning confocal microscopy; NOX, NADPH oxidase; PB, peripheral blood; PHD, prolyl hydroxylase; pVHL, von Hippel-Lindau protein; RNS, reactive nitrogen species; ROS, reactive oxygen species

2. Materials and methods

2.1. Cell samples

Peripheral blood (PB)-HSCs were obtained from healthy donors for allogeneic transplantation after informed consent. Mobilization of HSCs from BM by G-CSF-treatment was performed as in [12] and

CD34+ or CD133+ immuno-selection following apheresis as in [12,13]. The purity of the isolated cells was routinely >98% [12] and their viability, determined by trypan blue exclusion, was typically between 80% and 95%. Lymphomononuclear (LMN) cells were isolated from peripheral heparinized venous blood by density-gradient sedimentation over Ficoll–Paque. EA.hy926, a hybridoma cell line derived by fusing primary human umbilical vein endothelial cells (HUVEC) with the permanent human cell line A549 (lung carcinoma), was grown in Dulbecco's minimum essential medium (DMEM) containing 10% FBS.

2.2. Immuno-cytochemistry and laser scanning confocal microscopy (LSCM) analysis

PB-HSC samples (3×10^6/ml) and LMN were cyto-centrifuged on poly-lysine coated slides, fixed, permeabilized, blocked [as in [14]] and incubated with 1:50 diluted mouse mAb anti-human HIF-1α (Santa Cruz) overnight at 4 °C. Staining of EA cells was carried out under identical conditions directly on glass bottom dishes. After two washes in PBS, the samples were incubated with 8 μg/ml of the fluorescein isothiocyanate (FITC)- or rhodamine-labelled goat anti-mouse IgG (Santa Cruz). In the double staining experiments, the cells were incubated simultaneously with the mouse anti-HIF1α and 1:50 diluted rabbit anti-human pVHL (Santa Cruz) overnight at 4 °C, followed by 1 h incubation with FITC-labelled goat anti-mouse IgG and tetramethyl-rhodamine isothiocyanate (TRITC)-labelled goat anti-rabbit IgG (Santa Cruz), added sequentially. Imaging of labelled cells was performed by a Nikon TE 2000 microscope (images collected using a 60× objective 1.4 NA) coupled to a Radiance 2100 dual laser scanning confocal microscopy system (Biorad). The fluorescent signals emitted by the FITC-conjugated Ab (λex, 490 nm; λem, 525 nm) and by TRITC-conjugated secondary Ab (λex, 543 nm; λem, 572 nm) were from confocal planes of 0.2 μm in thickness examined along the z-axes, going from the top to the bottom of the cells. Acquisition, storage and analysis of data were made using LaserSharp and LaserPix software from Biorad and Image J.

2.3. Analysis of HIF-1α protein by immunoblotting

5×10^7 cells/ml were suspended in ice-cold lysis buffer (20 mM HEPES, pH 7.2, 150 mM NaCl, 1 mM EGTA, 10% glycerol, 1% Triton X-100, 1.5 mM $MgCl_2$, 2 mM sodium phosphate, and protease inhibitor cocktail). Lysates were centrifuged at 12000 rpm for 15 min at 4 °C and 60 μg of the supernatants were suspended in Laemmli's buffer and run on a 10% SDS–PAGE followed by Western-blotting. After the transferring procedure, the membrane was blocked with 10% FBS in TTBS (10 mM Tris–HCl, 150 mM NaCl, 0.1% tween 20 pH 8) for 1 h at 37 °C and subsequently incubated with the 1:300 diluted mouse mAb anti-HIF-1α (Santa Cruz) or 1:10000 diluted mouse anti-β-actin (Sigma) overnight at 4 °C. The membrane was washed three times with TTBS and incubated for 1 h at room temperature with the diluted 1:3000 horseradish peroxidase-conjugated secondary antibody (Santa Cruz). Subsequently, the membrane was washed three times with TTBS, analyzed by chemiluminescence (Amersham) and visualized with the VersaDoc Imaging System (Bio-Rad) by Quantity One software.

2.4. Reverse transcription-polymerase chain reaction

Total cellular RNA (3 μg) isolated by Trizol reagent was reverse transcribed to cDNA with specific antisense primers (50 pmol each) following the SuperScript Reverse Transcriptase protocol. Samples of 5 μL of RT reaction were PCR-amplified in a total volume of 50 μl with 50 pmol each of sense and antisense primers. The primer sequences were HIF1-α, forward (f)-5′-CTCAAAGTCGGACAGCCT-CA-3′, reverse (r)-5′-CCCTGCAGTAGGTTTCTGCT-3′ (460 bp); β-actin, f-5′-ACCAACTGGGACGACATGGAG-3′, r-5′-CGTGAG-GATCTTCATGAGGTACTC-3′ (35 bp). The conditions were 35 cycles of denaturation at 94 °C (1 min), annealing at 60 °C (1 min), and extension at 72 °C (2 min) followed by a further 10 min of extension. Purified PCR products were sequenced (three times for each sample) on an automatic ABI Prism 310 DNA sequencer.

For quantitative RT-PCR, prior to reverse transcription, RNA was subjected to DNAse (Ambion) treatment to remove contaminating genomic DNA. First strand cDNA synthesis was carried out using 300 ng of random hexamer primers by Superscript II (Invitrogen), starting from 300 ng RNA. Real-time quantification was performed with 2.5 μl cDNA using iQ SYBR Green Supermix (BIO-RAD) in 25 μl reaction volumes on an iCycler iQ detection system (BIO-RAD, Hercules, CA, USA) with 300 nM forward and reverse primer (VHL: f-5′-GAGTACGGCCCTGAAGAAGA-3′, r-5′-GCGATTG-CAGAAGATGACCT-3′; β-actin: 5′-TGGACATCCGCAAA-GACCTG-3′, r-5′-GCCGATCCACACGGAGTACTT-3′) and the following cycling steps: initial denaturation for 3 min at 94 °C, followed by 45 cycles with 15 s at 94 °C, 30 s at 60 °C and 10 s at 72 °C and 10 min terminal elongation at 72 °C. Melting curve analysis and agarose gel electrophoresis were performed to confirm the specificity of the amplification products. The relative quantification of transcript abundance in HSCs and LMNs was determined using the ΔΔCt method using β-actin as an internal standard. Two technical repeats per biological sample were analyzed. The efficiency of amplification, determined by serial dilutions of templates, was close to 100% for both transcripts and the liner regression coefficients were ⩾ 0.997.

2.5. HIF-1 DNA-binding assay

HIF-1 binding to a hypoxia responsive element (HRE) was assessed using the Trans-AM HIF transcription factor assay kit (Active) Motif Europe). Twenty micrograms of protein from cell lysates were analyzed for HIF-1 binding to an oligonucleotide containing the HIF-1 binding site from the erythropoietin (EPO) gene, according to the manufacturer's instructions using enzyme-linked immunosorbent assay technology with absorbance reading.

2.6. Flow cytometry

To measure reactive oxygen species (ROS) production, 10^6 cells were incubated with 10 μM 2′,7′-dichlorodihydrofluorescein-diacetate (H_2DCFDA) at 37 °C, protected from light for 30 min, in the presence of 20 μM cyclosporin A (CsA) [14]. After loading with dye, the cells were washed, resuspended in PBS and analyzed by a Beckman Coulter Epics XL-MCL flow cytometer equipped with a 488 nm Argon laser following the instrumental procedure (λem, 529 nm). The emitted fluorescent signal was acquired and analyzed with Expo 32 ADC software and was relative to 10000 events for each sample.

2.7. Statistical analysis

The two tailed Student's t-test was applied to evaluate the significance of differences measured throughout the data-sets reported. Significant differences were considered when $P < 0.05$.

3. Results

3.1. PB-HSCs express a stabilized form of HIF-1α under normoxic conditions

In this study, the analysis was carried out on freshly isolated HSC samples, deliberately avoiding any further manipulation (i.e. culturing) to keep the cells as close as possible to their physiological state. Two immuno-selection procedures were employed based on the CD34 and CD133 markers, the latter ensuing in a cell population enriched in more primitive HSCs [15].

Fig. 1A shows the result of a LSCM–immuno-cytochemistry inspection to detect the presence of HIF-1α. It can be noted that either the CD133- and CD34-PB-HSCs displayed a clear intracellular fluorescence documenting the possible expression of the HIF-1α protein. The fluorescent signal appeared mainly localized in the thin extra-nuclear cytoplasmic rim (≈80% of the total intracellular signal) as shown by imaging analysis of median confocal planes along the z-axis (Fig. 1B). Similar results were obtained for mobilized-HSCs from different donors (8–10 HSC-sample preparations) and confirmed by using a different HIF-1α-epitope-specific mAb (data not shown).

This observation, somehow surprising because it revealed the presence of a stabilized form of the HIF-1α protein under normoxic conditions (i.e. room air partial oxygen pressure),
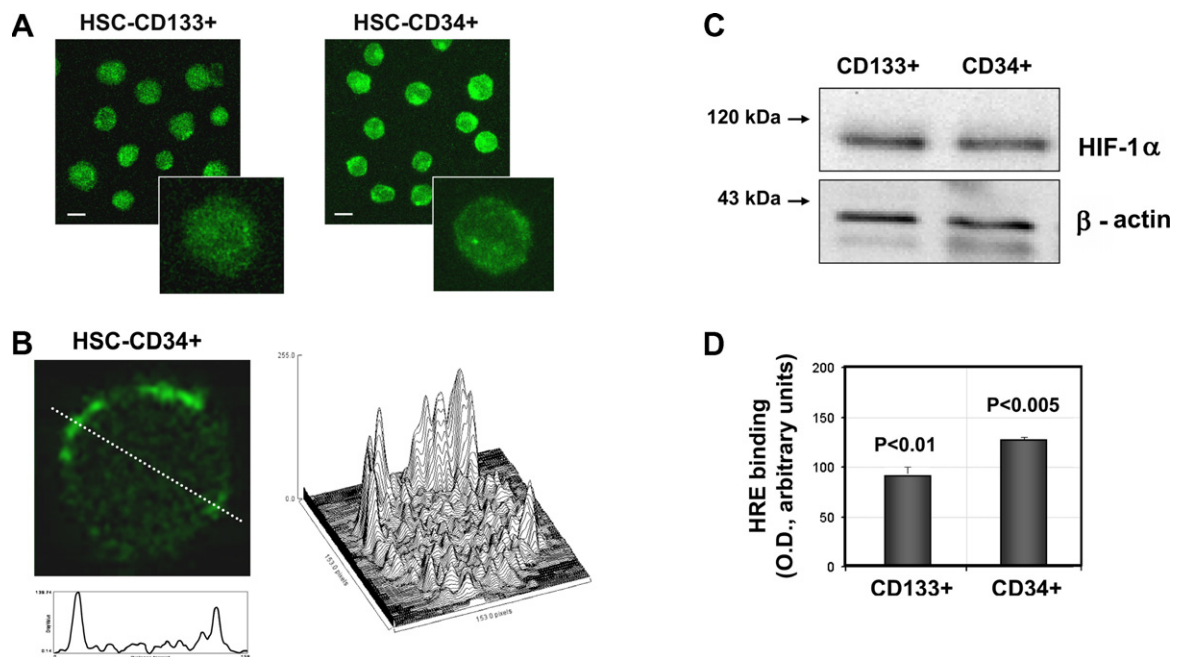
Fig. 1. PB-HSCs express stable HIF-1α protein under normoxic conditions. (A) and (B) LSCM analysis for immuno-cytochemistry detection of HIF-1α.The secondary Ab was FITC-conjugated and, when used on cell samples without the primary mAb, did not result in any detectable staining (not shown). In (A) the images are the result of superimposed confocal planes and are representative of at least four different preparations for each HSC sample. Bars: 10 μm. Enlargements of single cell imaging are also shown for either CD34+ and CD133+ HSC samples. In (B), analysis of a single confocal plane for a median section along the z-axis is shown (representative of >30 single CD34+HSC analysis). The pixel density profile is given along a line crossing the cell section and as a surface plot of the whole image. (C) immunoblotting of HIF-1α from cell lysates. (D) ELISA test of HIF-1 DNA-binding assay of cell extracts; average (±S.E.M.) of 3–4 different experiments with the reported P-value referring to the blank assessing the specificity of the assay system. See Section 2 for further experimental details.

was validated by immunoblotting in the PB-HSC total protein extract (Fig. 1C). Moreover, the binding of protein cell-lysate to an HRE-containing oligonucleotide, where HIF-1α specifically binds, was assayed and resulted in semi-quantitative ELISA readings that were statistically different from the blank assessing the specificity of the assay system (Fig. 1D).

Double immuno-cytochemistry of PB-HSCs for HIF-1α and CD34 showed that more than 95% of HSCs possessing stabilized HIF-1α were also CD34 positive, with a slight positive correlation between the two antigens (data not shown). This result indicated that the observed normoxic stabilization of HIF-1α was a feature shared among all the PB-HSCs and not confined to a cellular subset.

3.2. Normoxic stabilization of HIF-1α in PB-HSCs CD34+ occurs at the post-translational levels and is not further affected by conditions mimicking hypoxia

In Fig. 2, a survey aimed at better characterizing the features of HIF-1α in PB-HSC/CD34+ is presented. Identical analysis was carried out on isolated human LMN and cultured EA cells. The former was taken as an example of terminally differentiated blood cells along the myeloid and lymphoid lineages, whereas the latter was chosen because it is widely utilized to study the regulation of HIF-1α. Fig. 2A shows that, unlike PB-HSCs, immunoblotting for HIF-1α resulted in an undetectable amount of the protein, for both LMN and EA cells, whereas the mRNA transcription levels were comparable in all the three cell samples assayed. The absence of the HIF-1α protein in normoxic LMN and EA cells was also confirmed by immuno-chemical LSCM analysis (Fig. 2B). Furthermore,

the observation of any significant binding to HRE from LMN and EA cell extracts corroborated the absence of evidence in them for HIF-1α normoxic stabilization (Fig. 2C).

Fig. 2B, C shows, in addition, that treatment of LMN and EA cell samples with desferrioxamine (DFX), a condition mimicking hypoxia [16], induced stabilization of HIF-1α in LMN and EA, but did not result in any further significant effect on PB-HSCs when assayed by either immuno-cytochemistry or blotting (Fig. 2B). Moreover, the DNA-binding assay confirmed the DFX-induction of functional HIF-1 in LMN and EA cells (Fig. 2C). Treatment of HSC, LMN and EA cells with DFX did not cause any appreciable change in the HIF-1a transcript level (tested by RT-PCR, data not shown). These observations showed that our detection system was fully appropriate and that HSCs expressed constitutively HIF-1α under normoxia at a level comparable with that exhibited by other cell-types under hypoxia-like conditions. Therefore the presence of HIF-1α in mobilized normoxic HSCs was likely due to post-translational stabilization rather than to enhanced transcription.

3.3. Expression levels of HIF-1α and pVHL are inversely correlated in CD34+ PB-HSCs

As rapid proteasome degradation of HIF-1α under normoxic conditions is known to be driven by the intervention of the tumour suppressor pVHL [17], we next investigated its expression level by immuno-cytochemistry. Fig. 3A shows a representative LSCM analysis of PB-HSC/CD34+ sample co-stained for immuno-fluorescence detection of both HIF-1α and pVHL. A heterogeneous population of cellular subsets is
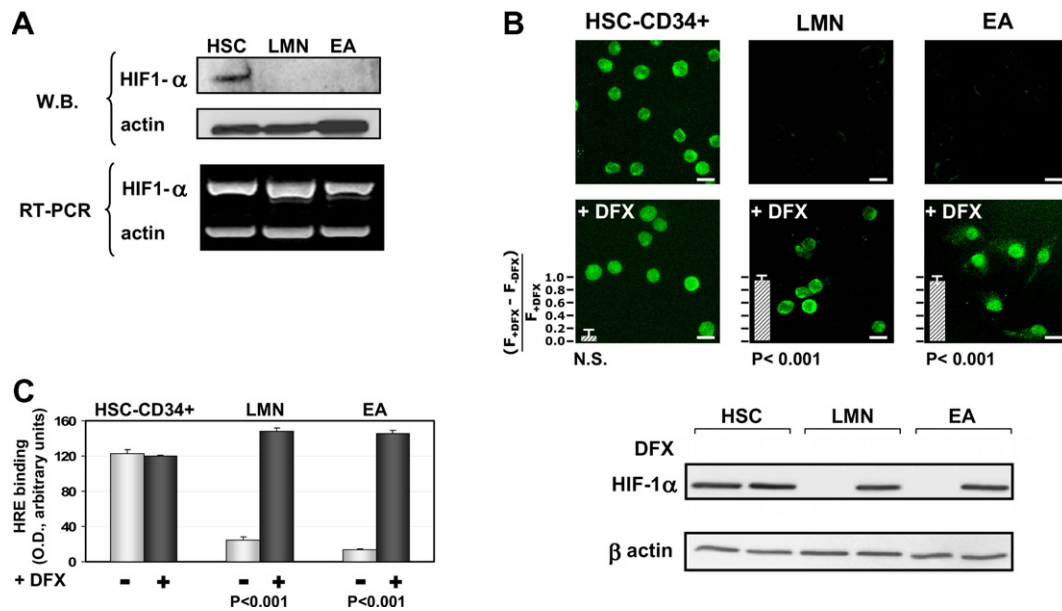
Fig. 2. Conditions mimicking hypoxia do not result in extra-stabilization of HIF-1α in PB-HSCs. (A) immunoblotting and mRNA expression of HIF-1α in cell lysates from PB-CD34+HSCs, lymphomonocytes (LMN) and an endothelial-derived cell line (EA). (B) Laser scanning confocal analysis for immuno-cytochemistry detection of HIF-1α in PB-HSCsCD34+, LMN and EA under normoxic conditions and following 12 h treatment with 10 mM desferrioxamine (DFX). Representative experiments out of four are shown. Immuno-cytochemistry, as in Fig. 1A. The quantitative analysis of the normalized fluorescence increase caused by DFX treatment (i.e. $(F_{+DFX} - F_{-DFX})/F_{+DFX}$) is displayed as bars ($\pm$S.E.M.; $n = 4$ for each condition) superimposed on the LSMC images along with statistical evaluation. The effect of DFX treatment on the HIF-1α protein level is also shown as immunoblotting of the protein extract from the three cell-types (bottom part of the panel; representative of three experiments). (C) Effect of DFX treatment on the HIF-1 DNA-binding assay; average ($\pm$S.E.M.) of 3–4 different experiments. NS: not significant. See Section 2 for further experimental details.

evident in most of the cells displaying high levels of HIF-1α and scant levels of pVHL, whereas others had high levels of pVHL and practically no evidence of HIF-1α; besides these two opposites, cells expressing intermediate levels of the two proteins were detectable. A semi-quantitative analysis on single cells of the subsets' distribution revealed that more than 50% of the HSCs had a high level of stabilized HIF-1α and a hardly perceptible amount of pVHL. The transcription level of pVHL was tested by quantitative RT-PCR in different HSC samples and compared with that of the terminally differentiated LMN (Fig. 3B). It is shown that on an average basis, HSCs displayed a significantly lower level of pVHL transcript (42% of LMN). Taken together, these results showed that complete or partial stabililization of HIF-1α under normoxic conditions in the largest set of the PB-HSCs was due to a defective expression of pVHL.

3.4. HIF stability is controlled by NADPH-oxidase-dependent ROS production

Stabilization of HIF-1α under normoxia has been reported to be controlled by reactive oxygen and nitrogen species (ROS, RNS) [18,19]. The analysis, the results of which are reported in Fig. 4, was carried out to address this specific point. Fig. 4A shows that when assayed by flow-cytometry using the ROS sensitive DCF probe, PB-HSCs revealed a constitutive ROS production that was prevented by diphenylene iodinium (DPI), an inhibitor of FAD-containing oxidases [20]. An even stronger reduction of ROS production was attained upon treatment of the cell sample with DFX. In this case, the chelating effect of DFX is likely to abrogate the free iron-dependent ROS formation by the Fenton-like reaction. On the other hand, the generic NOS inhibitor, L-monomethyl-L-arginine

(L-NNMA), did not cause any effect on the ROS-producing activity of the pre-treated cell sample. Fig. 4B,C shows that treatment of HSC with DPI resulted in a 50% inhibition of the binding capacity of HIF-1α to its target DNA sequence and in an even more pronounced disappearance/degradation of the protein when assayed by LSCM–immuno-cytochemistry. Conversely, L-NAME and DFX did not produce any effect, either on the DNA-binding activity or on the stabilization of HIF-1α. As the effect of DPI was evident following incubations as short as 2 h, this result suggested a positive control by ROS on the stabilization of HIF-1α at the post-translational rather than transcriptional level. This conclusion was verified and validated by immunoblotting analysis (Fig. 4D) showing a substantial decrease of the HIF-1α protein level following DPI-treatment. The well-documented inhibitory effect of DFX on the prolyl-hydroxylases (PHDs) can explain its failure in destabilizing HIF-1α, notwithstanding the observed large abrogation of ROS. This strongly indicates that the HIF-1α-stabilization-effect of ROS is mediated by their action on the catalytic efficiency of PHDs. Fig. 4E shows that the effect of DPI was mimicked by apocynin (a more specific inhibitor of NADPH oxidase) but not by treatment of HSC with rotenone *plus* antimycin A. The latter, when used together, inhibit ROS-generation by the mitochondrial respiratory chain, whose involvement in the stabilization of HIF-1α could therefore be ruled out.

4. Discussion

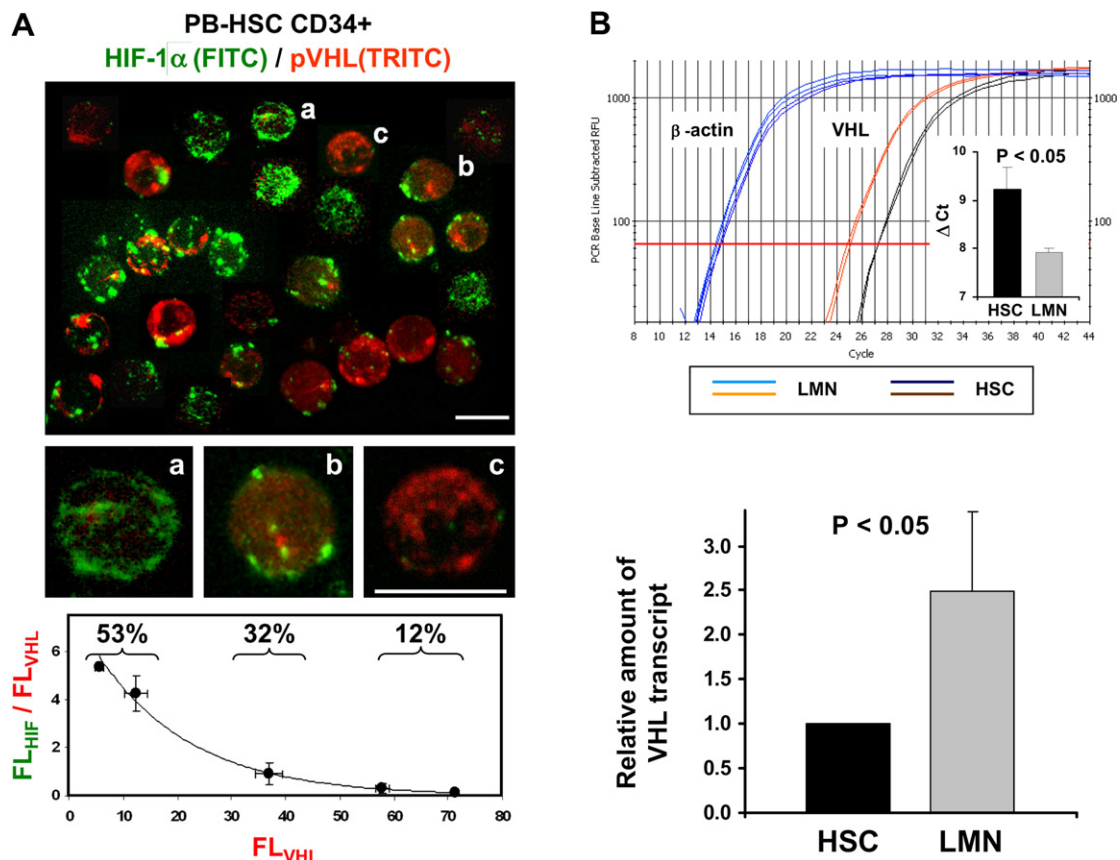Stabilization of HIF-1α is controlled by two well-defined linked mechanisms: hydroxylation of specific residues and pro-

Fig. 3. Expression levels of HIF-1α and pVHL are inversely correlated in PB-HSCs CD34+. (A) LSCM analysis of PB-CD34+HSCs for double immuno-cytochemistry detection of HIF-1α and pVHL. HIF-1α was green fluorescent labelled with FITC-conjugated Ab, pVHL was red fluorescent labelled with a TRITC-conjugated secondary Ab; (a–c) are enlarged images of selected cells representative of subsets. A representative experiment out of three is shown. Bars: 10 μm. Lower panel: quantitative correlation between the fluorescence intensity of FITC- and TRITC-conjugated secondary Abs bound to primary anti-HIF-1α and anti-pVHL, respectively. The values shown are averages (±S.D.) of clustered single cell image analyses comprising around 100 randomly selected different cells. The indicated percentage represents the calculated subset of cell distribution. (B) Comparative quantitative RT-PCR assay for the pVHL mRNA in HSC and LMN. Upper panel: amplification plot representative of four assays performed with different HSC and LMN samples. The inset shows the statistical analysis for the ΔCt values of VHL vs β-actin amplicons for either cell-type. Lower panel: relative amount of the VHL transcripts in HSCs and LMNs estimated by the ΔΔCt method with respect to the housekeeping β-actin gene transcript and normalized to the LMN value (average ±S.E.M. from four different HSC samples. See Section 2 for further experimental details.

teasomal degradation. Prolyl-hydroxylases are di-oxygenases that mediate post-translational modification of two conserved proline residues in HIF-1α at positions 402 and 564 [21]. Under normoxia, HIF-1α is prolyl-hydroxylated and as such, provides recognition sites for the binding of the pVHL. This tumour suppressor, once bound to HIF-1α, recruits the E3 ubiquitin ligase complex and promotes its extensive ubiquitination and targeting to proteasome degradation [17,22]. The affinity of PHD for O_2 is such that when its concentration falls below 3%, it becomes limiting and therefore, the pVHL-mediated degradation is strongly reduced. Consequently, HIF accumulates and can translocate into the nucleus where it forms, with its partner HIF-1β, a hetero-dimer able to bind HREs on promoters or enhancer regions. Unlike most nucleus-imported proteins, which require the common importins α or β, nuclear translocation of HIF-1α is mediated by different importin isoforms, which bind peculiar nuclear localization sequences (NLS) of HIF-1α [23]. A limiting expression of these specific nuclear translocation factors in HSCs might explain the predominant extracellular localization of HIF-1α under normoxia reported herein. Of note, full gene-transactivation

by HIF also depends on the recruitment of coactivators (like P300/CBP, SRC-1, Ref-1), which is negatively regulated by hydroxylation of aspargine 803, the target of another specific prolyl-hydroxylase (FIH, factor inhibiting HIF-1α) [24].

Therefore, stabilization of HIF-1α can be achieved by either limiting the availability of pVHL or desensitizing PHD to O_2-activation. These two features are both matched in the evidence provided in the present study. Indeed, immuno-cytochemistry analysis with an antibody recognizing pVHL failed to detect the protein in all but a limited subset of CD34+ PB-HSCs and, moreover, the cellular distribution of the HIF-1α was inversely related to the expression of pVHL. This is evocative of what has been observed in a number of cancerous cells where the absence of an active pVHL is associated with enhanced HIF-related vasculogenesis activity [25]. To our knowledge, the sole report of a physiological down-regulation of pVHL concerns human cytotrophoblast stem cells during uterine invasion under normoxia [26]. Unlike the shortage of information about the O_2-regulation of pVHL, the desensitization under normoxia of PHDs is amply documented. Reactive oxygen and nitrogen species (ROS, RNS) have been
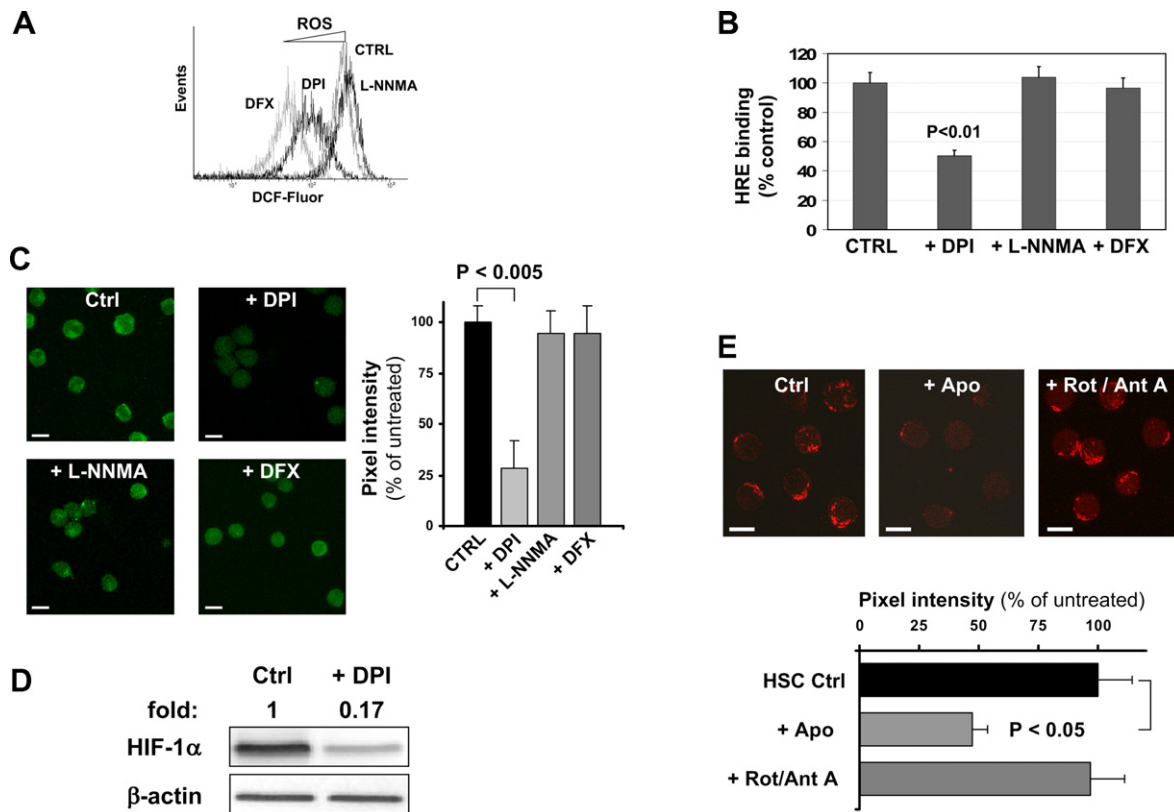
Fig. 4. HIF stability is controlled in PB-HSCs by NADPH-oxidase-dependent ROS production. Effect of DPI, DFX and L-NNMA on: (A) intracellular ROS production, assayed by flow cytometry with dichlorofluorescein (DCF); (B) HIF-1 DNA-binding assay; (C) immuno-cytochemistry detection of HIF-1α by confocal microscopy. HSCs were incubated with 20 μM DPI or 10 mM DFX or 1 mM L-NNMA for 2 h at 37 °C. (D) Effect of DPI-treatment on HIF-1α protein assayed by immunoblotting. The fold increase of the HIF-1α protein following DPI-treatment and assayed by densitometry of the HIF-1a band normalized to β-actin and to the untreated HSC sample (Ctrl) is shown (representative of three experiments yielding similar results). (E) Effect of 100 μM apocynin or 2 μM rotenone + 1μM Antimycin A on HIF-1α LSCM–immuno-cytochemistry (incubation conditions for the inhibitors as for A–D). In (C) and (D), the secondary Ab was conjugated with FITC and rhodamine, respectively, and the quantitative analysis of the fluorescence expressed as percentage of that in untreated HSCs (Ctrl) is displayed as bars ($\pm$S.E.M.; $n = 4$ for each condition) along with statistical evaluation. White bars, 10 μm.

shown to enhance stabilization of HIF-1α [18,19]. Although the mechanism of inhibition has not yet been fully elucidated, two feasible modalities of action have been proposed. ROS and RNS can directly ligate to the active ferrous iron center of PHDs (altering its redox properties) and/or may promote phosphorylation-dependent stabilization of HIF-1α [27]. In these latter cases, ROS and RNS would function as second messengers, possibly due to their well-documented inhibitory action on protein phosphatase activity [28].

In a previous work, we showed that HSCs are endowed with a constitutively active NADPH oxidase, which generates low-regiment ROS [14]. Here, we show that inhibition of ROS production by DPI-treatment causes a marked destabilization of HIF-1α. RNS, on the other hand, do not seem to be involved in HIF stabilization, as treatment of PB-HSC with an inhibitor of the NOS-synthase(s) was ineffective.

A very recent report has shown that glycogen synthase kinase 3 (GSK3) phosphorylates HIF-1a in the oxygen-dependent domain (ODD) leading to its proteasome degradation via a VHL-independent mechanism [29]. Activation of the protein kinase B (PKB) pathway, which phosphorylates and inactivates GSK3, promotes HIF-1a stabilization. Notably, ROS are well-known activators of the PKB pathway, and thus, elevation of intracellular ROS might mediate stabilization of

HIF-1a via this newly discovered additional mechanism, besides that controlling the PHD/VHL system. If this alternative mechanism is operative in HSCs, it might explain our observation that reduction of ROS by DPI-treatment causes substantial degradation of HIF-1a in all of the cell populations, including the VHL-deficient subset.

The reported affinity for O_2 of NADPH oxidase (NOX) ($K_m \approx 10$ μM) [30] enables ROS production efficiency to be sensitive to the physiological range of O_2 concentration experienced by HSCs when passing from BM (5–15 μM O_2) to PB (40–50 μM O_2) [5]. However, the absence of a stabilized HIF-1α protein in isolated BM-resident HSCs (also expressing NOX isoforms like in PB-HSCs [Piccoli et al., unpublished results]) when assayed under normoxic conditions (data not shown), strongly suggests that factors other than the level of O_2 are involved. It might well be that mobilization of BM-residing HSCs by G-CSF-treatment promotes events linked to stabilization of HIF. Of note, recent observations indicate that G-CSF binding to its cognate receptor on myeloid cell-types causes an increase of ROS production by at least two modalities. One involves the Lyn-PI 3K-kinase-Akt cascade [31], and the other, the ferritin-labile iron pool pathway [32]. Moreover, it has been reported that some of the gene products controlled by HIF (like EPO) stimulate ROS production as
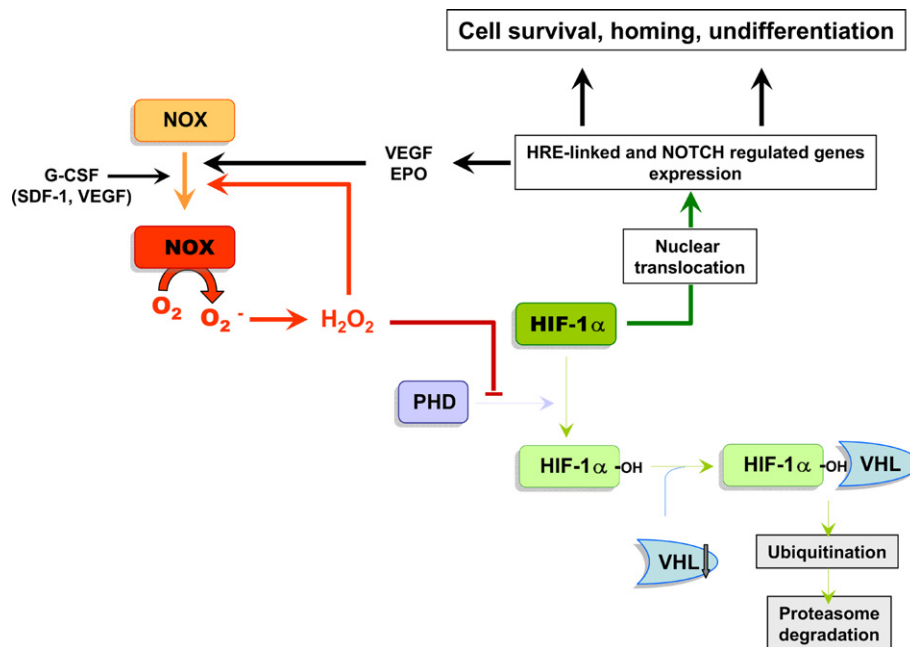
Fig. 5. Scheme showing the proposed mechanism for HIF-1α stabilization in mobilized HSCs under normoxic conditions. The initial event leading to activation of NOX is proposed to be linked to the chemokine (G-CSF or SDF-1) signal transduction pathway. Consequent increase of ROS would cause stabilization of HIF-1α under normoxic conditions, likely via inhibition of prolyl-hydroxylases (PHD). Nuclear translocation of HIF-1α promoting the trans-activation of HRE-linked genes might support cell survival and, in addition, sustain via an autocrine mechanism a positive feedback loop for redox signalling. Moreover, binding of HIF-1α to Notch regulated genes would activate the expression of specialization-suppressing genes favouring maintenance of the uncommitted state. See Section 4 for further explanation.

well [33]. So the effect of G-CSF could be to prime HSC to NOX-dependent ROS production, and activation of HIF would turn in an autocrine positive feed-back mechanism of maintenance under normoxia [34–36]. A working model illustrating the possible mechanism of HIF-1α stabilization under normoxia in PB-HSCs is shown in Fig. 5; the obvious question remaining to be answered concerns its physiological meaning.

Although speculative, it is tempting to make suggestions based on the latest reports. A very recent study carried out in HIF-1α-knock out mice showed that HIF-1α deficiency caused hematopoietic defects downstream of multipotential myeloid progenitors, which were more pronounced in the committed erythroid progenitors [37]. Moreover, the finding that the homozygosis condition of the pVHL R200W mutation causes Chuvash polycytemia [38] supports the critical role of HIF in promoting survival, proliferation and differentiation of hematopoietic progenitors. One further possibility is that HIF stabilization may represent a sort of pre-conditioning, conferring an advantage for homing of BM-mobilized HSCs to hypoxic tissues preserving at the same time the undifferentiation state. Hypoxic tissues, like peri-ischemic areas in the heart, have been shown to promote a larger HSC mobilization by release of stromal-derived factor (SDF-1), which acts at the level of bone marrow, recruiting in the circulating blood undifferentiated HSCs [10,39]. Following a chemotactic gradient, HSCs can reach the hypoxic tissue and provide therein a source of endothelial precursors that could help in the re-vascularization process, as recently suggested by a study showing that endothelial cells are an intrinsic component of adult myeloid lineage differentiation [40]. Given the inter-changeable features shared by chemokines and growth factors [41], it is possible that G-CSF conditioning might mimic the physiolog-

ical BM-mobilization of HSCs [42] under emergency conditions.

Very recent observations have provided a molecular mechanism for the inhibition of hypoxia on terminal differentiation of stem cells. It has been reported that HIF-1α binds to the cleaved intracellular domain of Notch and is recruited to the promoter regions of Notch-responsive genes [43]. Activation of Notch signalling makes available repressors that down-regulate specialization genes. Consistent with this observation, hypoxia maintains the expression of pref-1, a key stem/precursor cell gene that negatively regulates adipogenic differentiation by a mechanism in which HIF-1α has been demonstrated to be involved [44].

In summary, the data here presented show, for the first time, that human PB-HSCs CD133+/CD34+ are endowed with a system enabling the stabilization of HIF-1α under normoxic conditions. Our results indicate that two mechanisms would contribute to HIF stabilization: one is based on the constitutive NOX-dependent ROS generation which likely inhibits PHDs, the other on the down-regulation in the expression of pVHL in a subset of PB-HSCs. Chemokine-dependent mobilization from the bone marrow of HSCs is suggested to be the event triggering activation of HIF, which then is self-maintained by a redox-dependent positive feed-back regulation. In view of the recently recognized role played by HIF in controlling maintenance of the undifferentiated state in stem/progenitor cells, our finding might have possible applications in regenerative medicine.

References

[1] Iyer, N.V., Kotch, L.E., Agani, F., Leung, S.W., Laughner, E., Wenger, R.H., Gassmann, M., Gearhart, J.D., Lawler, A.M., Yu, A.Y. and Semenza, G.L. (1998) Cellular and developmental control of O₂ homeostasis by hypoxia-inducible factor 1 alpha. Genes Dev. 12, 149–162.

[2] Maxwell, P.H. (2005) Hypoxia-inducible factor as a physiological regulator. Exp. Physiol. 90, 791–797.

[3] Semenza, G.L. (1998) Hypoxia-inducible factor 1: master regulator of O₂ homeostasis. Curr. Opin. Genet. Dev. 8, 588–594.

[4] Kaelin, W.G. (2005) Proline hydroxylation and gene expression. Annu. Rev. Biochem. 74, 115–128.

[5] Chow, D.C., Wenning, L.A., Miller, W.M. and Papoutsakis, E.T. (2001) Modeling pO(2) distributions in the bone marrow hematopoietic compartment. I. Krogh's model. Biophys. J. 81, 675–684.

[6] Li, Z. and Li, L. (2006) Understanding hematopoietic stem-cell microenvironments. Trends Biochem. Sci. 31, 589–595.

[7] Scadden, D.T. (2006) The stem-cell niche as an entity of action. Nature 441, 1075–1079.

[8] Csete, M. (2005) Oxygen in the cultivation of stem cells. Ann. NY Acad. Sci. 1049, 1–8.

[9] Kim, C.G., Lee, J.J., Jung, D.Y., Jeon, J., Heo, H.S., Kang, H.C., Shin, J.H., Cho, Y.S., Cha, K.J., Kim, C.G., Do, B.R., Kim, K.S. and Kim, H.S. (2006) Profiling of differentially expressed genes in human stem cells by cDNA microarray. Mol. Cells 21, 343–355.

[10] Ceradini, D.J., Kulkarni, A.R., Callaghan, M.J., Tepper, O.M., Bastidas, N., Kleinman, M.E., Capla, J.M., Galiano, R.D., Levine, J.P. and Gurtner, G.C. (2004) Progenitor cell trafficking is regulated by hypoxic gradients through HIF-1 induction of SDF-1. Nat. Med. 10, 858–864.

[11] Dery, M.A., Michaud, M.D. and Richard, D.E. (2005) Hypoxia-inducible factor 1: regulation by hypoxic and non-hypoxic activators. Int. J. Biochem. Cell Biol. 37, 535–540.

[12] Tabilio, A., Falzetti, F., Giannoni, C., Aversa, F., Martelli, M.P., Rossetti, M., Caputo, P., Chionne, F., Gambelunghe, C. and Martelli, M.F. (1997) Stem cell mobilization in normal donors. J. Hematother. 6, 227–234.

[13] Aversa, F., Tabilio, A., Velardi, A., Cunningham, I., Terenzi, A., Falzetti, F., Ruggeri, L., Barbabietola, G., Aristei, C., Latini, P., Reisner, Y. and Martelli, M.F. (1998) Treatment of high-risk acute leukemia with T-cell-depleted stem cells from related donors with one fully mismatched HLA haplotype. New Engl. J. Med. 339, 1186–1193.

[14] Piccoli, C., Ria, R., Scrima, R., Cela, O., D'Aprile, A., Boffoli, D., Falzetti, F., Tabilio, A. and Capitanio, N. (2005) Characterization of mitochondrial and extra-mitochondrial oxygen consuming reactions in human hematopoietic stem cells. Novel evidence of the occurrence of NAD(P)H oxidase activity. J. Biol. Chem. 280, 26467–26476.

[15] Kobari, L., Giarratana, M.C., Pflumio, F., Izac, B., Coulombel, L. and Douay, L. (2001) CD133+ cell selection is an alternative to CD34+ cell selection for ex vivo expansion of hematopoietic stem cells. J. Hematother. Stem Cell Res. 10, 273–281.

[16] Wang, G.L. and Semenza, G.L. (1993) Desferrioxamine induces erythropoietin gene expression and hypoxia-inducible factor 1 DNA-binding activity: implications for models of hypoxia signal transduction. Blood 82, 3610–3615.

[17] Cockman, M.E., Masson, N., Mole, D.R., Jaakkola, P., Chang, G.W., Clifford, S.C., Maher, E.R., Pugh, C.W., Ratcliffe, P.J. and Maxwell, P.H. (2000) Hypoxia inducible factor-alpha binding and ubiquitylation by the von Hippel-Lindau tumor suppressor protein. J. Biol. Chem. 275, 25733–25741.

[18] Kietzmann, T. and Gorlach, A. (2005) Reactive oxygen species in the control of hypoxia-inducible factor-mediated gene expression. Semin. Cell Dev. Biol. 16, 474–486.

[19] Kasuno, K., Takabuchi, S., Fukuda, K., Kizaka-Kondoh, S., Yodoi, J., Adachi, T., Semenza, G.L. and Hirota, K. (2004) Nitric oxide induces hypoxia-inducible factor 1 activation that is dependent on MAPK and phosphatidylinositol 3-kinase signaling. J. Biol. Chem. 279, 2550–2558.

[20] Morre, D.J. (2002) Preferential inhibition of the plasma membrane NADH oxidase (NOX) activity by diphenyleneiodonium chloride with NADPH as donor. Antioxid. Redox Signal. 4, 207–212.

[21] Epstein, A.C., Gleadle, J.M., McNeill, L.A., Hewitson, K.S., O'Rourke, J., Mole, D.R., Mukherji, M., Metzen, E., Wilson, M.I., Dhanda, A., Tian, Y.M., Masson, N., Hamilton, D.L., Jaakkola, P., Barstead, R., Hodgkin, J., Maxwell, P.H., Pugh, C.W., Schofield, C.J. and Ratcliffe, P.J. (2001) C. elegans EGL-9 and mammalian homologs define a family of dioxygenases that regulate HIF by prolyl hydroxylation. Cell 107, 43–54.

[22] Maxwell, P.H., Wiesener, M.S., Chang, G.W., Clifford, S.C., Vaux, E.C., Cockman, M.E., Wykoff, C.C., Pugh, C.W., Maher, E.R. and Ratcliffe, P.J. (1999) The tumour suppressor protein VHL targets hypoxia-inducible factors for oxygen-dependent proteolysis. Nature 399, 271–275.

[23] Depping, R., Schindler, S., Friedrich, B., Sommer, N., Hartmann, E., Jelkmann, W., Metzen, E. and Koehler, M. (2005) Nuclear translocation of hypoxia-sensing transcription factors: involvement of the importin alpha/beta-system. FEBS J. 272 (s1), G3–011P.

[24] Lando, D., Peet, D.J., Gorman, J.J., Whelan, D.A., Whitelaw, M.L. and Bruick, R.K. (2002) FIH-1 is an asparaginyl hydroxylase enzyme that regulates the transcriptional activity of hypoxia-inducible factor. Genes Dev. 16, 1466–1471.

[25] Kim, W.Y. and Kaelin, W.G. (2004) Role of VHL gene mutation in human cancer. J. Clin. Oncol. 22, 4991–5004.

[26] Genbacev, O., Krtolica, A., Kaelin, W. and Fisher, S.J. (2001) Human cytotrophoblast expression of the von Hippel-Lindau protein is downregulated during uterine invasion in situ and upregulated by hypoxia in vitro. Dev. Biol. 233, 526–536.

[27] Mazure, N.M., Brahimi-Horn, M.C. and Pouyssegur, J. (2003) Protein kinases and the hypoxia-inducible factor-1, two switches in angiogenesis. Curr. Pharm. Des. 9, 531–541.

[28] Chiarugi, P. (2005) PTPs versus PTKs: the redox side of the coin. Free Radic. Res. 39, 353–364.

[29] Flugel, D., Gorlach, A., Michielis, C. and Kietzmann, T. (2007) Glycogen synthase kinase 3 phosphorylates hypoxia-inducible factor 1a and mediates its destabilization in a VHL-independent manner. Mol. Cell Biol. 27, 3253–3265.

[30] Koshkin, V. (1995) Aerobic and anaerobic functioning of superoxide-producing cytochrome b-559 reconstituted with phospholipids. Biochim. Biophys. Acta 1232, 225–229.

[31] Zhu, Q.S., Xia, L., Mills, G.B., Lowell, C.A., Touw, I.P. and Corey, S.J. (2005) G-CSF induced reactive oxygen species involves Lyn-PI 3-kinase-Akt and contributes to myeloid cell growth. Blood 107, 1847–1856.

[32] Yuan, X., Cong, Y., Hao, J., Shan, Y., Zhao, Z., Wang, S. and Chen, J. (2004) Regulation of LIP level and ROS formation through interaction of H-ferritin with G-CSF receptor. J. Mol. Biol. 339, 131–144.

[33] Iiyama, M., Kakihana, K., Kurosu, T. and Miura, O. (2006) Reactive oxygen species generated by hematopoietic cytokines play roles in activation of receptor-mediated signaling and in cell cycle progression. Cell Signal. 18, 174–182.

[34] Janowska-Wieczorek, A., Majka, M., Ratajczak, J. and Ratajczak, M.Z. (2001) Autocrine/paracrine mechanisms in human hematopoiesis. Stem Cells 19, 99–107.

[35] Kirito, K., Fox, N., Komatsu, N. and Kaushansky, K. (2005) Thrombopoietin enhances expression of vascular endothelial growth factor (VEGF) in primitive hematopoietic cells through induction of HIF-1alpha. Blood 105, 4258–4263.

[36] Mayer, H., Bertram, H., Lindenmaier, W., Korff, T., Weber, H. and Weich, H. (2005) Vascular endothelial growth factor (VEGF-A) expression in human mesenchymal stem cells: autocrine and paracrine role on osteoblastic and endothelial differentiation. J. Cell Biochem. 95, 827–839.

[37] Yoon, D., Pastore, Y.D., Divoky, V., Liu, E., Mlodnicka, A.E., Rainey, K., Ponka, P., Semenza, G.L., Schumacher, A. and Prchal, J.T. (2006) Hypoxia-inducible factor-1 deficiency results in dysregulated erythropoiesis signaling and iron homeostasis in mouse development. J. Biol. Chem. 281, 25703–25711.

[38] Ang, S.O., Chen, H., Hirota, K., Gordeuk, V.R., Jelinek, J., Guan, Y., Liu, E., Sergueeva, A.I., Miasnikova, G.Y., Mole, D., Maxwell, P.H., Stockton, D.W., Semenza, G.L. and Prchal, J.T. (2002) Disruption of oxygen homeostasis underlies congenital Chuvash polycythemia. Nat. Genet. 32, 614–621.

[39] Ceradini, D.J. and Gurtner, G.C. (2005) Homing to hypoxia: HIF-1 as a mediator of progenitor cell recruitment to injured tissue. Trends Cardiovasc. Med. 15, 57–63.

[40] Bailey, A.S., Willenbring, H., Jiang, S., Anderson, D.A., Schroeder, D.A., Wong, M.H., Grompe, M. and Fleming, W.H. (2006) Myeloid lineage progenitors give rise to vascular endothelium. Proc. Natl. Acad. Sci. USA 103, 13156–13161.

[41] Vandervelde, S., van Luyn, M.J., Tio, R.A. and Harmsen, M.C. (2005) Signaling factors in stem cell-mediated repair of infarcted myocardium. J. Mol. Cell Cardiol. 39, 363–376.

[42] Powell, T.M., Paul, J.D., Hill, J.M., Thompson, M., Benjamin, M., Rodrigo, M., McCoy, J.P., Read, E.J., Khuu, H.M., Leitman, S.F., Finkel, T. and Cannon 3rd, R.O. (2005) Granulocyte colony-stimulating factor mobilizes functional endothelial progenitor cells in patients with coronary artery disease. Arterioscler. Thromb. Vasc. Biol. 25, 296–301.

[43] Gustafsson, M.V., Zheng, X., Pereira, T., Gradin, K., Jin, S., Lundkvist, J., Ruas, J.L., Poellinger, L., Lendahl, U. and Bondesson, M. (2005) Hypoxia requires notch signaling to maintain the undifferentiated cell state. Dev. Cell 9, 617–628.

[44] Lin, Q., Lee, Y-J., Yun, Z. Differentiation arrest by hypoxia. J. Biol. Chem. doi:10.1074/jbc.C600120200.